

# High SBS-threshold single-mode single-frequency monolithic pulsed fiber laser in the C-band

Wei Shi<sup>\*1</sup>, Eliot B. Petersen<sup>1,2</sup>, Matthew Leigh<sup>1,3</sup>, Jie Zong<sup>1</sup>, Zhidong Yao<sup>1</sup>, Arturo Chavez-Pirson<sup>1</sup>, and Nasser Peyghambarian<sup>1,3</sup>

<sup>1</sup>NP Photonics Inc., 9030 S. Rita Road, Tucson, AZ, 85747, USA

<sup>2</sup>Physics Department, University of Arizona, Tucson, AZ 85721, USA

<sup>3</sup>College of Optical Sciences, University of Arizona, Tucson, AZ 85721, USA

\*Corresponding Author: [wshi@np Photonics.com](mailto:wshi@np Photonics.com)

**Abstract:** We report a high SBS-threshold, single-frequency, single-mode, polarization maintaining (PM) monolithic pulsed fiber laser source in master oscillator and power amplifier (MOPA) configuration that can operate over the C-band. In order to achieve a narrow transform-limited linewidth for pulses longer than 100 ns, we use a single-frequency Q-switched fiber laser seed, which itself can be seamlessly tuned up to 1.24  $\mu$ s. The Q-switched pulses are amplified in the power amplifier stage of MOPA using a high SBS threshold single-mode PM large core highly Er/Yb co-doped phosphate glass fiber (LC-EYPhF). This seed and amplifier combination represents the first monolithic, all-fiber implementation of a single-frequency pulsed laser with the highest pulse energy of 54  $\mu$ J and peak power of 332 W for 153-ns pulses at 1538 nm.

©2009 Optical Society of America

**OCIS codes:** (060.2320) Fiber optics amplifiers and oscillators; (140.3510) Lasers, fiber; (140.3480) Lasers, diode-pumped; (140.3538) Lasers, pulsed

---

## References and links

1. M. Stephen, M. Krainak, H. Riris, and G. R. Allan, "Narrowband, tunable, frequency-doubled, erbium-doped fiber-amplified transmitter," *Opt. Lett.* **32**, 2073-2075 (2007).
2. C. E. Dille, M. A. Stephen, and M. P. Savage-Leuchs, "High SBS-threshold, narrowband, erbium co-doped with ytterbium fiber amplifier pulses frequency-doubled to 770 nm," *Opt. Express* **15**, 14389-14395 (2007).
3. W. Shi, M. Leigh, J. Zong, Z. Yao, and S. Jiang, "Power scaling for narrow linewidth C-band pulsed fiber lasers using a highly Er/Yb co-doped phosphate glass fiber," *SPIE Photonics West 2008, OPTO, Optical Components and Materials V*, **19-24**, 6890-20 (2008).
4. B. Steinhäusser, A. Brignon, E. Lallier, J. P. Huignard, P. Georges, "High energy, single-mode, narrow-linewidth fiber laser source using stimulated Brillouin scattering beam cleanup," *Opt. Express*, **15**, 6464-6469 (2007).
5. V. Philippov, C. Codemard, Y. Jeong, C. Alegria, J. K. Sahu, and J. Nilsson, "High-energy in-fiber pulse amplification for coherent lidar applications," *Opt. Lett.* **29**, 2590-2592 (2004).
6. G. P. Agrawal, *Nonlinear Fiber Optics*, Third Edition, (Academic, 2001).
7. M.-J. Li, X. Chen, J. Wang, S. Gray, A. Liu, J. A. Demeritt, A. B. Ruffin, A. M. Crowley, D. T. Walton, and L. A. Zenteno, "Al/Ge co-doped large mode area fiber with high SBS threshold," *Opt. Express*, **15**, 8290-8299 (2007).
8. J. Nilsson, "SBS Suppression at the kilowatt level," *SPIE Photonics West 2009*, 7195-50.
9. J. M. Fini, "Bend-resistant design of conventional and microstructure fibers with very large mode area," *Opt. Express* **14**, 69-81 (2006).
10. V. I. Kovalev and R. G. Harrison, "Suppression of stimulated Brillouin scattering in high-power single-frequency fiber amplifiers," *Opt. Lett.* **31**, 161-163 (2006).
11. N. G. R. Broderick, H. L. Offerhaus, D. J. Richardson, R. A. Sammut, J. Caplen, and L. Dong, "Large mode area fibers for high power applications," *Opt. Fiber Technol.* **5**, 185-196 (1999).
12. F. D. Teodoro, J. P. Kopolow, S. W. Moore, and D. A. V. Kliner, "Diffraction-limited, 300-kW peak-power pulses from a coiled multimode fiber amplifier," *Opt. Lett.* **27**, 518-520 (2002).
13. J. M. Fini, "Design of large-mode-area amplifier fibers resistant to bend-induced distortion," *J. Opt. Soc. Am. B* **24**, 1669-1676 (2007).
14. Y. Kaneda, Y. Hu, C. Spiegelberg, J. Geng, and S. Jiang, "Single-frequency, all-fiber Q-switched laser at 1550-nm," *OSA Topical Meeting on Advanced Solid-State Photonics 2004*, Postdeadline paper PD5

15. Y. Kaneda, C. Spiegelberg, J. Geng, and Y. Hu, "All-fiber Q-switched laser," Patent 7130319, 2006.
  16. W. Shi, M. A. Leigh, J. Zong, Z. Yao, A. Chavez-Pirson and N. Peyghambarian, "High power all fiber-based narrow linewidth single-mode fiber laser pulses in the C-band and frequency conversion to THz generation," *IEEE J. Sel. Top. Quantum Electron.* **15**, 377-384 (2009).
  17. W. Shi, M. Leigh, J. Zong, Z. Yao, and S. Jiang, "Photonic narrow linewidth GHz source based on highly co-doped phosphate glass fiber lasers in a single MOPA chain," *IEEE Photon. Technol. Lett.* **20**, 69-71 (2008).
  18. M. Leigh, W. Shi, J. Zong, Z. Yao, S. Jiang, and N. Peyghambarian, "High peak power single frequency ns pulses using a short phosphate glass fiber with a large core," *Appl. Phys. Lett.* **92**, 181108-181110 (2008).
  19. W. Shi, M. Leigh, J. Zong, and S. Jiang, "Single-frequency THz source pumped by Q-switched fiber lasers based on difference-frequency generation in GaSe crystal," *Opt. Lett.* **32**, 949-951 (2007).
  20. B. Ruffin, M.-J. Li, X. Chen, A. Kobayakov, and F. Annunziata, "Brillouin gain analysis for fibers with different refractive indices," *Opt. Lett.* **30**, 3123-3125 (2005).
  21. N. Peyghambarian and S. Jiang, "Erbium and ytterbium co-doped phosphate glass optical fiber amplifiers using short active fiber length," US Patent, 6611372, Aug 26, 2003.
  22. Y. Hu, S. Jiang, T. Luo, K. Seneschal, M. Morrell, F. Smektala, S. Honkanen, J. Lucas, and N. Peyghambarian, "Performance of high-concentration Er<sup>3+</sup>-Yb<sup>3+</sup>-codoped phosphate fiber amplifiers," *IEEE Photon. Technol. Lett.* **13**, 657-659 (2001).
  23. Y. W. Lee, K. E. Urbanek, M. J. F. Digonnet, R. L. Byer, and S. Jiang, "Measurement of the stimulated Brillouin scattering gain coefficient of a phosphate fibre," *Proc. SPIE* 6469, 64690L (2007).
- 

## 1. Introduction

Fiber lasers pumped by semiconductor lasers are becoming more and more important in laser applications. Monolithic all fiber-based pulsed fiber lasers are particularly promising sources for laser sensing, imagery, velocimetry, anemometry, and coherent LIDAR owing to their high spatial and spectral qualities, as well as their rugged, compact, maintenance-free, efficient, lightweight, and high beam quality features. For applications involving spectroscopic sensing and LIDAR, a high precision measurement highly depends on the linewidth or coherence length of the fiber laser pulses. For example, for active remote sensing spectroscopy, the oxygen absorption linewidth at standard temperature and pressure is in the range of a few gigahertz [1-2], so the linewidth and stability of the laser should be less than 10 MHz for high precision (fractions of a percent) measurements of the absorption lineshape and strength. Therefore, it is highly desirable to have fiber laser pulses with transform-limited linewidth, and pulse duration in 100 ns-500 ns range. In order to achieve a narrow linewidth pulsed fiber laser seed, it is possible to modulate a distributed feedback fiber laser (DFBL) or a single-frequency fiber laser by using electro-optic modulator or acoustic modulator [1-2, 3-5]. However, both of these approaches are bulky, expensive, and inefficient. In this paper, we report on single-frequency fiber laser pulses covering the nanosecond time regime obtained by using actively Q-switched fiber laser. This is the first demonstration of an all fiber-based Q-switched fiber laser with transform-limited linewidth that extends over such a wide and tunable pulse duration range of 7.5 ns - 1.24  $\mu$ s to the best of our knowledge. In addition, it is more efficient, compact and less expensive compared with the modulated fiber laser pulses.

For sub-microsecond pulses with single spatial mode and very narrow linewidth, the laser power scaling has been difficult in fiber amplifiers due to limitations primarily from the stimulated Brillouin scattering (SBS) nonlinear effect [1-3]. SBS builds up strongly in the fiber for narrow linewidth pulses of long pulse duration [6]. So it has been difficult to achieve high peak power, single-mode, and narrow linewidth operation simultaneously in a fiber laser system, especially for a monolithic master oscillator and power amplifier (MOPA) structure. Therefore, increasing the SBS threshold for the fiber amplifiers is crucial to scaling the peak and average power for the SM PM narrow linewidth sub-microsecond fiber laser pulses. There are three main approaches to reducing the SBS effect or increasing SBS threshold. One is to reduce the transverse overlap integral between the optical and acoustic fields as accomplished by proper profile design [7-8]. However, this approach is more effective for passive fiber than for large mode area (LMA) active fibers. The second is using a temperature gradient [9] or strain gradient [10] to essentially shorten interaction length by altering the SBS spectrum along the fiber. The last one that is the well-known approach to reduce the SBS effect is to make fibers with LMA [11]. The mode area is increased by lowering the core

numerical aperture (NA) and increasing the core diameter. However, the challenge is to decrease the core NA. For example, for the lowest commercial core NA of 0.06 the fiber is still multimode in the c-band when the core diameter is larger than 20  $\mu\text{m}$ . Single mode operations can be achieved by modal discrimination induced by coiling the fiber [12-13]. A side effect of this method is that for large core size, bending deforms the mode field distribution and thus reduces the mode area. In this paper, we demonstrate a high SBS threshold all-fiber based amplifier by using a single-mode PM large core highly Er/Yb co-doped phosphate glass fiber (LC-EYPhF) in the power amplifier stage of a monolithic MOPA configuration. The LC-EYPhF has high gain per unit length due to the high co-doped concentration. This is a unique feature of this active phosphate glass fiber. Also, we achieve low core NA  $\sim 0.053$  as a result of our precise control of core and cladding glass refractive indices and our unique rod-in-tube fiber drawing technique [14-18]. Previously, we have scaled the peak power of short ns pulses with transform-limited linewidth to more than 50 kW at  $\sim 1550$  nm and repetition rate of 5 kHz [18].

We believe that the demonstration of an all-fiber based solution in this operating regime is important for wider deployment of these laser systems in many applications such as coherent LIDAR where the all-fiber construction enables robust, maintenance-free, and high performance operation.

## 2. Single-frequency Q-switched fiber laser

Recently, we have developed an all fiber-based Q-switching laser using fiber stress birefringence induced by a piezo [14-17, 19]. In this method, a piece of piezo compresses a fiber creating stress birefringence, and this birefringence acts as a waveplate, changing the polarization state of the light in the fiber. This Q-switch mechanism is similar to using an electro-optic modulator, where the polarization is modulated to switch the laser between high and low feedback states. The cavity of our laser consists of NP Photonics' proprietary highly Er/Yb co-doped phosphate glass fiber, serving as the gain medium. The high doping concentration creates a strongly absorbing active fiber, allowing for a  $\sim 5$  cm cavity length that is significantly shorter than other Q-switched fiber lasers, which can have cavity lengths of meters to kilometers. This short cavity length creates large longitudinal mode spacing, helping to maintain lasing on a single longitudinal mode. The active fiber is spliced between two fiber Bragg gratings (FBGs) and a short section of standard non-PM fiber. A wavelength-stabilized 980 nm diode laser pumps the cavity. This configuration allows a laser cavity where there is no coupling to external bulk components such as acousto-optic modulators, while also eliminating fiber components within the cavity. The two fiber Bragg gratings act as cavity mirrors. The high reflector is written in a standard non-PM fiber, and has a fairly broad reflection band of 0.31 nm FWHM. The output coupler has a  $\sim 50\%$  transmission grating with a narrow linewidth of 0.03 nm FWHM. The use of FBGs permits thermal tuning of the laser by heating each grating. Because the OC-FBG is written in a PM fiber, the reflection band is split approximately 0.3 nm due to the different indices of refraction in the fast and slow axis of the PM fiber. We selected these gratings so the fast axis reflection would be within the reflection band of the HR-FBG while the slow axis would be located outside the reflection band. This creates a polarization-dependent cavity where the fast axis will have optical feedback and the slow axis will not. The polarization-dependent reflection permits Q-switching if the internal birefringence of the cavity can be modulated. We can control the polarization in the cavity by using a 2 mm long piezoelectric element to stress the fiber, with the compression axis rotated  $45^\circ$  relative to the axis of the PM fiber. This stress-induced birefringence acts as a waveplate, which rotates the polarization of the light inside the laser.

Figure 1(a) shows the pulse width variation with the repetition rate for the Q-switched fiber laser at 1550.67 nm when using 500-mW pump power at 980 nm. The shortest pulse width was 7.5 ns and occurred at a 5 kHz repetition rate when using a pump power of 500 mW. The highest peak power obtained was 15.32 W at repetition rate of  $\sim 20$  kHz, and the average power is from 0.014 mW to 18.78 mW for repetition rate of 50 Hz to 630 kHz. Figure 1(b) shows the pulse width variation with the pump power for the Q-switched fiber laser at

1538 nm at a repetition rate of 20 kHz. For other wavelengths in the c-band, the pulse width variations of the Q-switched fiber lasers with the repetition rate and pump power are very similar to that in Fig. 1. It is worth noting that the pulse width of the single-frequency Q-switched fiber laser pulses can be seamlessly tuned in a very wide range by tuning the repetition rate or the pump power. This is an important newly demonstrated capability of this fiber laser structure and design. One can see that the pulse duration can be easily tuned from 7.5 ns to 1.24  $\mu$ s by decreasing the pump power when using the fixed repetition rate of 20 kHz (see Fig. 1 (b)). Figure 2 shows the typical pulse shapes of the Q-switched fiber laser at 1538 nm with pulse widths of 15 ns, 145 ns and 162 ns, respectively. The solid curves are the measured temporal traces for the Q-switched pulses by using a fast oscilloscope and the dashed ones are the relative Gaussian fitting results. It is worth noting that the pulse shapes for the Q-switched pulses are all nearly Gaussian-like. Figure 3 shows the typical optical spectrum we measured by using an optical spectrum analyzer (OSA) with spectral resolution of 0.06 nm for the Q-switched fiber laser at 1538 nm. One can see the signal to noise ratio is close to 60 dB, which is a little bit lower than that of our standard CW single-frequency fiber laser (> 65 dB).

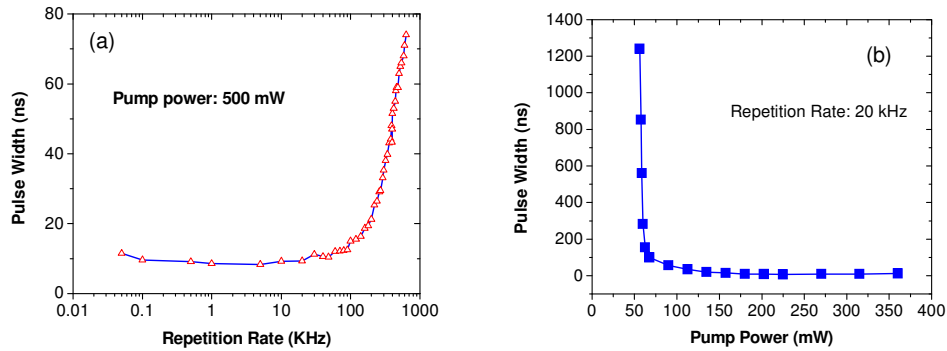


Fig. 1. (a). Pulse width variation with the repetition rate with pump power of 500 mW for 1550 nm fiber laser pulses, and (b) the pulse width variation with the pump power at a repetition rate of 20 kHz with the 1538 nm fiber laser pulses.

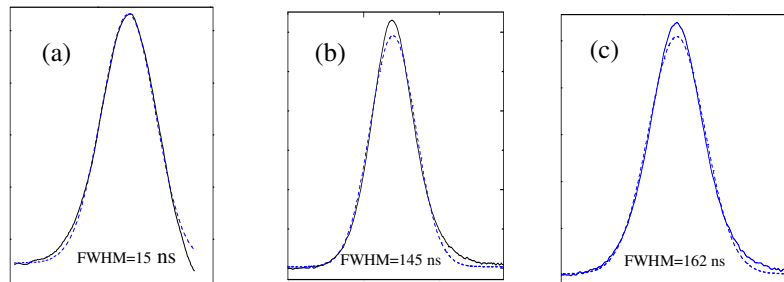


Fig. 2. The typical pulse shapes of the Q-switched fiber lasers with different pulse widths.

In order to estimate the linewidth of the Q-switched fiber laser, the laser spectra of the Q-switched laser at different pulse widths were measured by using a fiber-based scanning Fabry-Perot interferometer with a free spectral range (FSR) of 1 GHz and Finesse of  $\sim$ 198. Figures 4 (a) and 4(b) show the scanning spectra for 7.6 ns and 112 ns Q-switched fiber laser pulses. For the 7.6 ns pulses, the observed spectrum shows bursts of pulses under transmission peaks of

the Fabry-Perot, which are separated in time by the repetition rate of the laser. This observation confirms that the Q-switched fiber laser operates at a single frequency, and the linewidth of  $\sim 65$  MHz can be estimated by the envelope of the pulse train in the scanning Fabry-Perot spectrum for the related fiber laser pulses, which is very close to transform limited shown in Fig. 4(c). For the 112 ns pulses, the scanning Fabry-Perot spectrum shows the nearly single burst under transmission peaks of the Fabry-Perot, which corresponds to the line width of  $\sim 5$  MHz that is close to the bandwidth limit of the used Fabry-Perot interferometer. Therefore, for the Q-switched fiber laser pulses, it is expected that the linewidth is at least as small as  $\sim 5$  MHz when the pulse width is bigger than 112 ns.

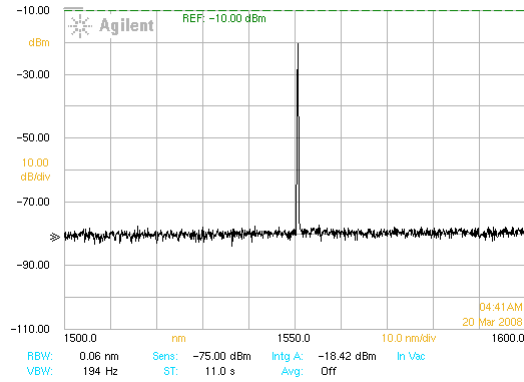


Fig. 3. Measured optical spectrum for the for the Q-switched fiber laser at 1538 nm

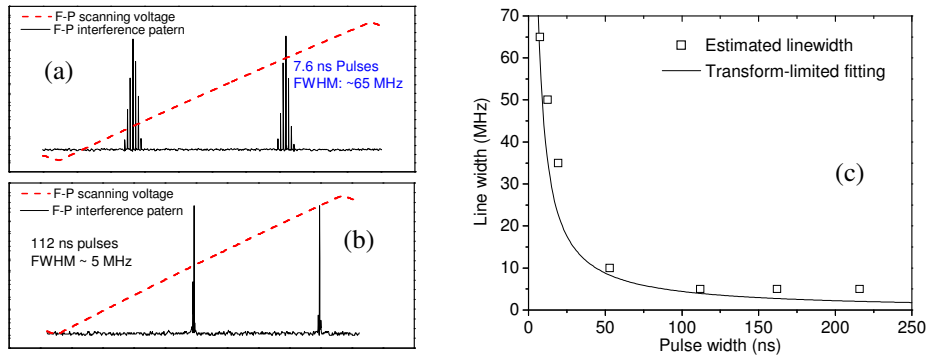


Fig. 4. Fabry-Perot scanning spectra of Q-switched fiber laser for (a) 7.6 ns pulses and (b) 112 ns pulses, and (c) estimated linewidths for Q-switched fiber laser pulses with different durations and the Gaussian transform-limited fitting.

### 3. Monolithic single-frequency pulsed fiber laser in MOPA

For longer ns pulses ( $>100$  ns) with single spatial mode and very narrow linewidth, the laser power scaling has been difficult in fiber amplifiers due to limitations primarily from the SBS nonlinear effect. This occurs because the pulse duration is much larger than the dephasing time ( $1/\pi\Delta\nu_{FWHM}$ ) that describes the time to phase the created phonons and build up the macroscopic acoustic wave in the material if we assume the Brillouin gain bandwidth  $\Delta\nu_{FWHM}$  is about 20 MHz at 1550 nm [1-3]. Therefore, increasing the SBS threshold for the fiber amplifiers is crucial to scaling the peak/average power for the SM PM narrow linewidth sub-microsecond fiber laser pulses.

In order to implement the high SBS-threshold amplifiers, we notice that the SBS threshold can be simply expressed as  $P_{SBS} \sim 21 \frac{A_{eff}}{K \cdot g_B L_{eff}}$  [6-7, 20], where  $A_{eff}$  is the optical effective mode area,  $g_B$  the Brillouin gain coefficient  $g_B = \frac{2\pi m^7 p_{12}^2}{c \lambda^2 V_s \Delta v_{FWHM}}$ ,  $L_{eff}$  the effective length of the active fiber ( $L_{eff} = \frac{1}{\exp(gL)} \int_0^L \exp(gz) dz$ , where  $g$  is the unit gain of the active fiber), and  $K$  the polarization dependence factor ( $1/3 < K < 2/3$  when  $L_{eff} \gg L_B$  where  $L_B$  is the polarization beating length). It is worth noting that our highly co-doping Er/Yb phosphate has the highest gain per unit length ( $> 5$  dB/cm) [16-19, 21-22]; resulting in a relative  $L_{eff}$  that is smaller one or two orders of magnitude than silica and silicate fibers. Furthermore, we have studied the SBS gain coefficient of our phosphate fibers [23], and determined that the SBS gain coefficient is only half of that of a silica fiber. According to the above analysis, we estimated the SBS threshold can be up to 2.8-5.6 kW for the 15  $\mu$ m core phosphate fiber LC-EYPhF with length of  $\sim 12$  cm.

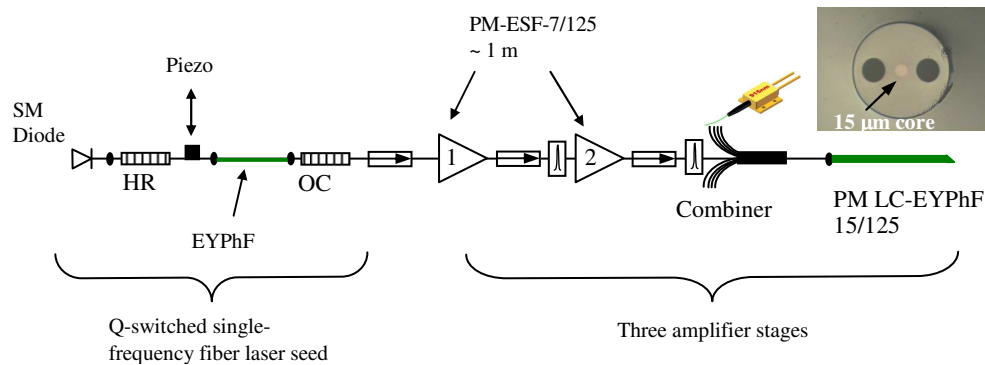


Fig. 5. Schematic of the SM single-frequency Q-switched fiber laser in MOPA.

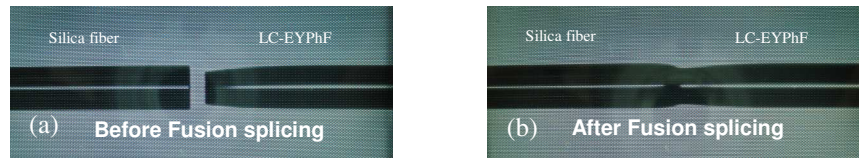


Fig. 6. Fusion splice processing of LC-EYPhF with commercial silica fiber

Figure 5 shows the schematic of the all fiber-based pulsed fiber laser source in MOPA, which uses LC-EYPhF with the optimized length of 12-cm in the power amplifier stage [16]. The single-frequency Q-switched fiber seed we used has a wavelength of 1538 nm, pulse duration of 160 ns, and repetition rate of 20 kHz. Two preamplifier stages used 1-m long commercial SM PM Er-doped active fibers (ESF-7/125), which were core pumped by using 980 nm SM diodes. We used three fiber-based PM isolators between the Q-switched single-frequency fiber laser seed and three amplifier stages in order to block the backward amplified spontaneous emission (ASE) and any reflection feedback. Between the three amplifier stages, we used two narrow band filters to further suppress the ASE component. In the power amplifier stage, the new developed SM PM Er/Yb highly co-doped ( $\sim 3\%Er-15\%Yb$ ) phosphate glass fiber LC-EYPhF was used, with a core diameter of 15  $\mu$ m, core NA of 0.053, and the cross section is shown as an inset of Fig. 5. The length of LC-EYPhF active fiber in the power amplifier is only 12 cm. The output end of the LC-EYPhF was angle polished in

order to minimize the end feedback. A commercial SM PM (6+1)×1 signal pump combiner was used to combine six commercial fiber pigtailed single emitters at 975 nm. The 12-cm EYPhF was arc fusion spliced with the silica fiber (output fiber) of the commercial combiner in-house using an asymmetric fusion splicing technique. Figure 6 shows the fusion splice processing of LC-EYPhF with commercial silica fiber. From Fig. 6 (a), one can see that the LC-EYPhF fiber with large core and low NA was tapered before fusion splicing in order to minimize the signal insertion loss of the fusion splicing by achieving the mode field diameter matching. The temperature and time should be very well controlled when tapering the LC-EYPhF fiber in order to avoid the adiabatic mode-field expansion. Figure 6(b) shows the fusion splicing joint by using the asymmetric fusion splicing technique through longitudinally offsetting the arc center. We want to point out that our filament fusion processing can do the above processes also, which generates the similar performance with arc fusion processing. However, the cost of the arc fusion processing is much lower than that of filament fusion processing currently.

#### 4. Experimental measurements and results

This pulsed fiber laser system can be operated in the whole C-band. In order to characterize the performance of the monolithic single-frequency Q-switched fiber laser in MOPA in Fig. 5, the single-frequency Q-switched fiber seed at wavelength of 1538 nm with pulse duration of 160 ns and repetition rate of 20 kHz was used. In this experiment, we kept the peak power after the 2<sup>nd</sup> amplifier below 30 W in order to avoid the SBS effect by monitoring the temporal pulse trace, OSA spectrum and Fabry-Perot scanning spectrum. For the SBS-free pulses after the 2<sup>nd</sup> amplifier, the pulse shape stays nearly the same as the Q-switched pulse seed before amplification. After the power amplifier stage, the pulse energy of the amplified fiber laser pulses was accurately measured by using a fast Ophir PE9F-SH pyroelectric energy meter that is accurate at repetition rates up to 20 KHz. This pulse energy meter is insensitive to the ASE background and CW signal component.

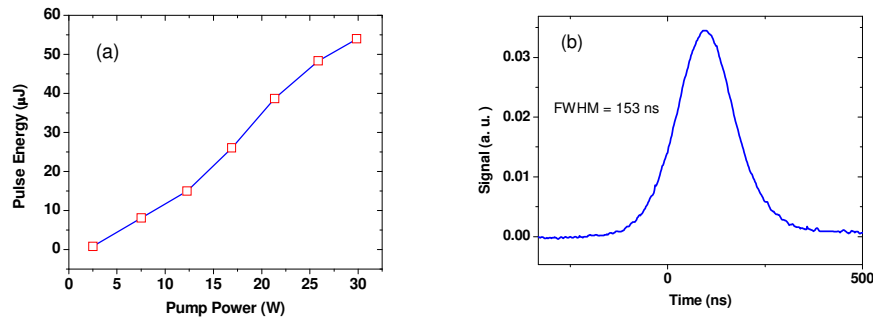


Fig. 7. (a). Pulse energy vs. power amplifier pump power for the MOPA system at ~ 1538 nm. (b). Typical pulse shape for the amplified 54 μJ pulses.

Figure 7(a) shows the typical pulse energy performance when different pump powers were used for the power amplifier of the MOPA system at ~ 1538 nm. When the average power of the input seed for the power amplifier stage was about 97.2 mW, the pulse energy was 4.86 μJ. Due to the high SBS threshold for the short length (~ 12 cm) LC-EYPhF in the amplifier stage, the pulse energy can be scaled up to 54 μJ with SBS-free when the pump power for the power amplifier stage is nearly 30 W.

Figure 7(b) shows the typical pulse shape for the power scaled pulses. One can see that the pulse duration was a little bit narrowed to ~ 153 ns for the 162 ns pulse seed. For Gaussian-like pulses, the peak power  $P_{peak}$  can be related to the pulse energy  $E$  as  $P_{peak} = \frac{E}{t_{FWHM}} 2\sqrt{\frac{\ln 2}{\pi}}$ . So the 54 μJ pulses correspond to a peak/average power of 332 W/1.08W at a repetition rate of

20k Hz. These pulse energy and peak power are the highest values to our knowledge for the monolithic single-frequency pulsed fiber lasers with longer ns pulse duration. The power gain for the power amplifier stage when using ~ 30 W pump power is about 10.5 dB corresponding to a unit gain of ~ 0.87 dB/cm.

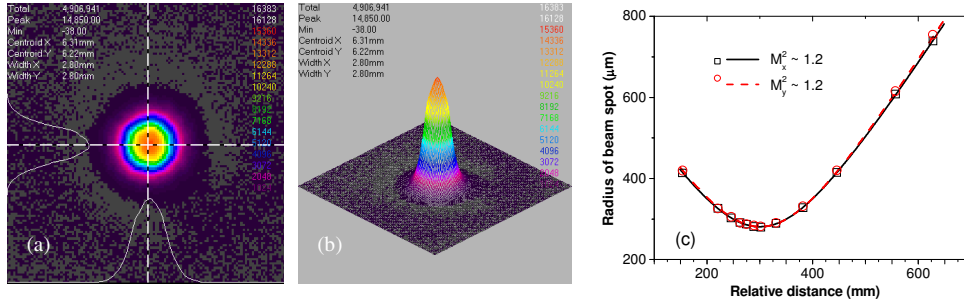


Fig. 8. (a) and (b), the images of the pulsed fiber laser profile displayed in 2D and 3D views for 54  $\mu$ J pulses; (c) Beam quality evaluation by measuring  $M^2$  values at two orthogonal directions by scanning the beam size around the waist position of the focused propagation beam.

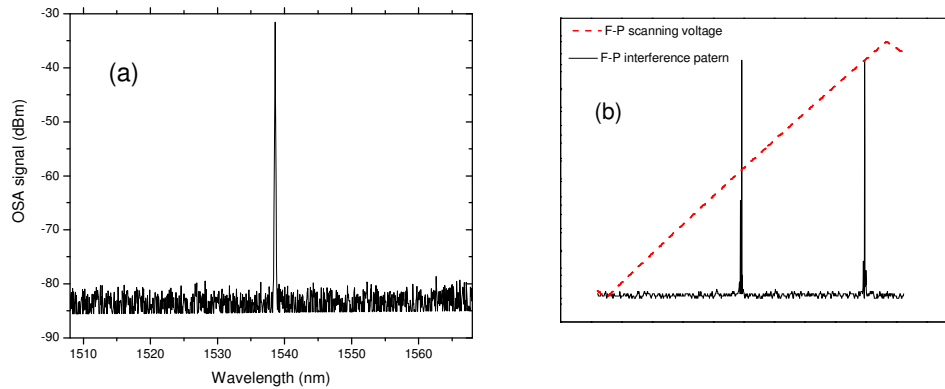


Fig. 9. (a), the spectral trace for 54  $\mu$ J pulses with 153 ns duration at 20 kHz repetition rate using an optical spectrum analyzer with a resolution of 0.06 nm; (b) the F-P scanning spectrum for 54  $\mu$ J pulses.

The output beam quality of the fiber laser pulses with 54  $\mu$ J per pulse was characterized by a Spiricon Pyrocam III. Figures 8(a) and 8(b) show the images of the pulsed fiber laser profile displayed in 2D and 3D views, which indicate the fiber laser pulses have diffraction limited beam quality. The beam quality was also evaluated by measuring the  $M^2$  values of around 1.2 for both vertical and horizontal directions through scanning the beam size around the waist position of the focused propagation beam, as shown in Fig. 8(c).

Figure 9(a) shows the spectral trace for 54  $\mu$ J pulses with 153 ns duration at 20 kHz repetition rate using an OSA with a resolution of 0.06 nm. One can see that these amplified SM pulses have a signal noise ratio of ~ 50 dB. From the F-P scanning spectrum in Fig. 9(b), it was estimated that the pulsed fiber laser in MOPA was operating in single-mode and the transform-limited linewidth is about 5 MHz. The measured polarization extinction ratio (PER) for the above amplified pulses is > 10 dB.

### 3. Conclusions

We have demonstrated a high SBS-threshold, single-frequency, SM PM monolithic pulsed fiber laser source based on a MOPA configuration that can operate over the C-band (1530nm-1565nm). The single-frequency pulsed fiber laser seed with longer ns pulses was achieved by using an actively Q-switched fiber laser, whose pulse duration can be tuned up to 1.24  $\mu$ s. This is an important newly demonstrated capability of this fiber laser structure and design. By using SM PM large core (15  $\mu$ m) highly Er/Yb co-doped phosphate glass fiber in the power amplifier stage in the all-fiber MOPA configuration, the pulse energy has been scaled up to 54  $\mu$ J for 153 ns pulses with an estimated linewidth of  $\sim$  5 MHz, corresponding to a peak power of 332 W without SBS effects. By using the Q-switched single-frequency fiber laser seed, this all-fiber based fiber laser MOPA system features compactness, simplicity, stability, and low cost, as well as performance marked by a high signal to noise ratio. These eye-safe high-energy all-fiber laser pulses with transform-limited linewidths are very important for applications involving range-finding, coherent LIDAR, and remote sensing after frequency doubling (e.g. the oxygen A band).

### Acknowledgments

This work has been funded by NASA and AFOSR under contracts FA9550-09-C-0060 and FA8650-09-M-5424. This research was also done as a collaborative program with the University of Arizona. Matthew Leigh is currently with Envisioneering, Inc. The UA part of the research was supported by an NSF ERC Cooperative Support Agreement Award No. EEC-0812072. The authors wish to thank Dr. Mark Stephen for fruitful discussions.